Lawrence Berkeley National Laboratory
Recent Work

Title

ATOMIC BEAM STUDY OF THE HYPERFINE STRUCTURE OF THULHM-170

Permalink

https://escholarship.org/uc/item/7d35402p

Authors

Cabezas, A.Y.
Lindgren, I.P.K.

Publication Date

1960-05-09

UNIVERSITY OF CALIFORNIA

Ernest O. Lawrence

Radiation Laboratory

BERKELEY, CALIFORNIA

DISCLAIMER

UNIVERSITY OF CALIFORNIA

Lawrence Radiation Laboratory
Berkeley, California

Contract No. W-7405-eng-48

ATOMIC BEAM STUDY OF THE HYPERFINE STRUCTURE OF THULIUM-170

A. Y. Cabezas and I. P. K. Lindgren

May 9, 1960

ATOMIC BEAM STUDY OF THE HYPERFINE STRUCTURE
OF THULIUM-170

A. Y. Cabezas and I. P. K. Lindgren

Lawrence Radiation Laboratory
University of California
Berkeley, California

May 9, 1960

ABSTRACT

The atomic-beam magnetic-resonance technique has been used to measure atomic and nuclear quantities of the 129-day isotope Tm^{170} as follows:

$$J = 7/2, \quad g_J = 1.14122 \pm 0.00015,$$

$$I = 1, \quad |A| = 200 \pm 3 \text{ Mc, and } |B| = 1010 \pm 15 \text{ Mc.}$$

The values of J and g_J are consistent with the ground-state assignment $^2F_{7/2}$. Values of the nuclear moments are calculated from the hyperfine-structure interaction constants A and B by use of a two-parameter radial wave function, in which one parameter is determined from comparison with Hartree functions and the other parameter from the experimental spin-orbit coupling constant. Uncorrected values are obtained, as follows:

$$|\mu_I| = 0.26 \pm 0.02 \text{ n.m. and } |Q| = 0.61 \pm 0.05 \text{ barns,}$$

with the two moments of the same sign. The same wave function is used to calculate the relativistic and diamagnetic corrections to the atomic g value, and the result is in excellent agreement with the experiment.

ATOMIC BEAM STUDY OF THE HYPERFINE STRUCTURE
OF THULIUM-170[*]

A. Y. Cabezas and I. P. K. Lindgren[†]

Lawrence Radiation Laboratory
University of California
Berkeley, California

May 9, 1960

INTRODUCTION

The work reported here is a part of a more general program for investigations of radioactive isotopes in the rare earth region (lanthanides) by the method of atomic beams. This technique involves hyperfine-structure (hfs) measurements and therefore gives information about the nucleus as well as the electronic structure. For the isotope reported here the nuclear spin (I), the magnetic dipole and electric quadrupole interaction constants (A, B), the total electronic angular momentum (J), and the atomic g value (g_J) have been measured.[1] From the hfs interaction constants approximate values of the nuclear moments have been calculated by use of an improved radial wave function.

This isotope has also been investigated by beta spectroscopists,[2] and their spin assignment is in agreement with ours.

The electronic ground state of thulium has been determined by optical methods,[3] and is (with spectroscopic notations) $4f^{13} 6s^2$, $^2F_{7/2}$, which is consistent with our results. The atomic g value, however, has not been accurately measured before, and is found to differ significantly from the classical Landé value. Since the state above is essentially a single-electron state the admixture of other states is very small. However, for a heavy atom like thulium the relativistic and diamagnetic effects become quite important. It is shown that when these effects are taken into account, as well as the anomalous moment of the electron, excellent agreement with the experimental g value is obtained.

EXPERIMENTAL METHOD AND RESULTS

The method employed in this experiment is the conventional atomic-beam flop-in technique, which has been described in detail in several articles.[4] The principles are briefly the following. A beam of free atoms is allowed to pass through a homogeneous magnetic field, and transitions are observed between different hfs levels. Transitions within the same F state are followed up from the linear Zeeman region, where they in principle give the nuclear spin, into intermediate fields, where information about the hfs is obtained. More accurate determinations of the hfs separations can then be made by observations of direct transitions between different F states.

The 129-day isotope Tm^{170} was produced by irradiation of thulium metal in a neutron flux of 2×10^{13} n/cm^2 · sec for a few weeks in the pool-type reactor at the Lawrence Radiation Laboratory, Livermore. The metal piece was then put directly into the tantalum oven of the atomic beam apparatus[5] and heated up to about 600 to 800°C. A few hundred milligrams was bombarded each time, and this gave a stable beam for several days. The beam was collected on clean platinum foils, which were subsequently counted in a continuous-flow proportional counter.

The Hamiltonian for a free atom in an external magnetic field $\bar{H}$ can be written[6]

$$\mathcal{H} = hA \, \bar{I} \cdot \bar{J} + hB \, Q_{op} - g_J \mu_0 \bar{J} \cdot \bar{H} - g_I \mu_0 \bar{I} \cdot \bar{H}, \qquad (1)$$

where

$$Q_{op} = \frac{3(\bar{I} \cdot \bar{J})^2 + 3/2(\bar{I} \cdot \bar{J}) - I(I+1) J(J+1)}{2I(2I-1) J(2J-1)} \quad .$$

Octupole and higher-order interactions are here omitted. The hfs energy

levels are shown schematically in Fig. 1 for Tm^{170} (I=1, J=7/2), in which

case there are three $\Delta F = 0$ transitions (α, β, γ) and two $\Delta F = 1$ transitions

(δ, ϵ) observable with a flop-in arrangement.

The energy levels at zero field are, from Eq. (1),

$$W_{9/2} = 7/2 \, hA + 1/4 \, hB,$$

$$W_{7/2} = -hA - 5/7 \, hB,$$

$$W_{5/2} = -9/2 \, hA + 15/28 \, hB.$$

The relative positions of these levels are shown in Fig. 2 as a function of

the ratio B/A. The level order is normal in the region $-4.667 < B/A < 2.8$.

The experimental ratio is -5.05, which means that the $F = 9/2$ and $F = 7/2$

levels are inverted. Since this ratio is very close to one of the critical

values, the two hfs separations become very different in magnitude (73 and

1960 Mc, respectively) and this gives the three $\Delta F = 0$ transitions quite

different behavior as the magnetic field increases. Figure 3 shows the

frequency divided by $\mu_0 H/h$ for these transitions. At low fields the fre-

quencies are approximately given by

$$\nu \cong g_F \, \frac{\mu_0 H}{h} \quad,$$

where

$$g_F \cong g_J \, \frac{F(F+1) - I(I+1) + J(J+1)}{2F(F+1)} \quad.$$

Therefore, in this diagram the curves start at the g_F values and have a

slope at the beginning corresponding to the second-order term. The alpha

transition has no quadratic term and actually starts with a zero slope.

Since the separation between $F = 9/2$ and $F = 7/2$ ($\Delta\nu_1$) is so small,

however, the higher-order terms become significant at a relatively low field.

Also, for the beta transition the higher-order terms very soon become predominant, and the total shift from the linearity turns negative. The gamma transition, on the other hand, is independent of $\Delta\nu_1$ in the first approximation and consequently has a much smaller relative shift. The points in Fig. 3 correspond to the experimental resonance frequencies, and the curves show the corresponding values calculated for the best fit of the three parameters a, b, and g_J.

The three $\Delta F = 0$ transitions have been followed up to about 300 gauss, and one of the $\Delta F = 1$ transitions, δ, has been observed at two low fields. The other $\Delta F = 1$ transition, ϵ, occurs at an inconveniently high frequency (approx 1960 Mc) and has not been looked for. The resonance curves for each of the $\Delta F = 0$ transitions at the highest field are shown in Fig. 4 together with one curve for the $\Delta F = 1$ transition. The latter transition is of σ type ($\Delta m = 0$) and the resonance curve is therefore double-peaked. The resonance frequency corresponds to the center of the dip. In general, the uncertainty in the resonance frequency has been taken to be about $\pm 1/4$ of the half-width of the resonance curve.

The experimental data have been analyzed on the IBM computer 704, with a program described elsewhere.[7] A least-square fit is made of the three parameters (a, b, and g_J) and also a correction for the small g_I term which appears in Eq. (1). The sign of the nuclear moment, however, has to be chosen in advance and can be determined only from comparison between the fits with opposite sign assumptions.

Figure 5 shows the input and output sheets from the computer. The input sheet gives all the resonance frequencies for both the radioactive isotope and the calibration isotope (K^{39}). The output sheet gives the best

values of a, b, and g_J, with uncertainties, and also the differences between the experimental and calculated frequencies as well as the χ^2 value for the best fit. A positive sign of the nuclear moment gives a smaller χ^2 but the difference is not significant. This means that the moment is too small to allow a definite sign determination from this experiment. However, the relative sign of the dipole and quadrupole moments can be uniquely determined from the sign of the B/A ratio.

The final results are

$$J = 7/2, \quad g_J = 1.14122 \pm .00015,$$

$$I = 1, \quad |A| = 200 \pm 3 \text{ Mc}, \quad |B| = 1010 \pm 15 \text{ Mc}, \quad (B/A < 0).$$

We have here stated larger errors than obtained from the computer in order to include possible systematic errors.

CALCULATION OF THE NUCLEAR MOMENTS

Since the electronic configuration of thulium consists of com-
pletely filled shells minus one electron, the relations between the hfs
interaction constants and the nuclear moments are given by[8]

$$A = c \, R_y \, a^2 \, g_I \frac{\ell(\ell+1)}{j(j+1)} \, F \left\langle \frac{a_0^3}{r^3} \right\rangle$$

(2)

$$B = -c \, R_y \, \frac{Q}{a_0^2} \, \frac{2j-1}{j+1} \, R \left\langle \frac{a_0^3}{r^3} \right\rangle \; ,$$

where R_y is the Rydberg constant, a the fine-structure constant, and a_0
the first Bohr radius. The relativistic correction factors F and R are
for f electrons very close to unity and are here discarded.

In order to estimate $\left\langle r^{-3} \right\rangle$ one needs some approximate radial
wave function. In most applications hydrogenic wave functions have been
used, but these cannot be expected to be good approximations, except for
electrons moving very close to the nucleus. This is clearly demonstrated
by self-consistent-field (SCF) calculations.

With the wave function discussed in the Appendix, which is a
modification of the hydrogenic wave function to better agreement with SCF
calculations, we get, in atomic units,

$$\kappa = 0.40 : \left\langle r^{-3} \right\rangle = 10.6,$$

$$\kappa = 0.44 : \left\langle r^{-3} \right\rangle = 10.4.$$

This shows, as one would expect, that the shape of the wave function is not
critical when $\left\langle r^{-3} \right\rangle$ is determined from the experimental spin-orbit coupling
constant. Ridley[9] gives for Tm^{3+} 11.5 au, which should be slightly higher
than for the neutral atom, since the removal of the outer electrons pushes

the other electrons a little closer to the nucleus. The very crude hydrogenic
formula for the spin-orbit coupling constant,

$$\zeta = hc\, R_y\, a^2\, Z_{eff} \left\langle r^{-3} \right\rangle = hc\, R_y\, a^2\, \frac{Z_{eff}^4}{n^3\, \ell(\ell+1/2)(\ell+1)},\qquad (3)$$

which is frequently used by spectroscopists, gives $\left\langle r^{-3} \right\rangle = 13.1$ au, which
is certainly too high.

With $\left\langle r^{-3} \right\rangle = 10.5$ au we get, for the nuclear moments (un-
corrected values)

$$|\mu_I| = 0.26 \pm 0.02 \text{ nm},$$

$$|Q| = 0.61 \pm 0.05 \text{ barns},$$

with the two moments of the same sign. The error in the magnetic moment
is large enough to include diamagnetic corrections. For the quadrupole
moment, on the other hand, corrections of the Sternheimer type,[10] which
have not been considered here, might make the corrected value fall outside
the given limits.

The hfs of the stable isotope Tm^{169} has been investigated optically
by Lindenberger,[11] and he gives for the magnetic moment

$$\mu_I^{169} = -0.20_5 \pm 0.02 \text{ nm}.$$

Although he uses hydrogenic wave functions, he gets, surprisingly enough,
consistent results from the hfs constants for the 4f and 6s electrons. With
our value of $\left\langle r^{-3} \right\rangle$ for the 4f electron, which we believe is more accurate,
we obtain from his data

$$\mu_I^{169} = -0.25 \text{ nm},$$

which is outside the given limits of error.

CORRECTIONS TO THE ATOMIC g VALUE

Since the ground state of thulium is essentially a single-electron state, the admixture of other states is very small. Furthermore, the electrostatic interaction can mix only states with the same S, L, and J and hence has no effect on the g value. An estimate of the configuration interaction caused by the spin-orbit coupling shows that its effect is quite negligible compared with the experimental uncertainty. Therefore, all the measurable deviation from the classical Landé value must be due to (a) the anomalous magnetic moment of the electron and (b) relativistic and diamagnetic effects. By relativistic effects we mean here the change of the interaction between the atomic moment and the external field, due to the velocity of the electron, and the change of the spin-orbit coupling, due to the external field. These corrections follow directly from the Dirac equation for a single electron, and are proportional to the kinetic energy T in the first approximation. The diamagnetic correction is caused by changes in the spin-other-orbit and orbit-orbit interactions, due to the external field. This correction depends essentially on the electron density in the core.

The relativistic correction to the magnetic moment of a single electron has been calculated by Breit[12] and Margenau[13] and can be written

$$\delta g_1 = a^2 \frac{(j + 1/2)^2}{j(j + 1)} \langle T \rangle . \tag{4}$$

All radial integrals are here expressed in atomic units. This correction is usually referred to as the Breit-Margenau correction.

In their discussion of the Zeeman effect in atomic oxygen Abragam and VanVleck[14] have calculated the diamagnetic correction, assuming spherically symmetric electron density. From their expressions we get

for the diamagnetic correction to the Zeeman energy for a single electron

in the state $(n \ \ell \ m_s \ m_\ell)$,

$$\delta Z = -\mu_0 H a^2 \left[(m_\ell + 2m_s) \langle Y \rangle - m_s \langle \sin^2 \theta \rangle \langle U \rangle \right], \tag{5}$$

where

$$U = \frac{1}{r^3} \int_0^r r'^2 \rho(r') dr', \quad Y = \frac{1}{3} \left[U + \int_r^\infty \frac{\rho(r')}{r'} dr' \right]$$

and

$$\langle \sin^2 \theta \rangle = 2 \ \frac{\ell(\ell+1) - 1 + m_\ell^2}{(2\ell-1)(2\ell+3)} \ .$$

Here $\rho(r')$ is the radial density of all electrons, except the one we are

taking the average for.

From Eqs. (4) and (5) we get the total correction for an f

electron in the state $^2F_{7/2}$,

$$\delta g = -a^2 \left[\frac{64}{63} \langle T \rangle + \frac{8}{7} \langle Y \rangle - \frac{8}{63} \langle U \rangle \right].$$

With the wave function described in the Appendix and the electron density

from the Thomas-Fermi model, we obtain the following values of the

radial integrals:

$$\kappa = 0.40 : \langle T \rangle = 24.7, \quad \langle U \rangle = 16.5, \quad \langle Y \rangle = 13.3 \text{ au;}$$

$$\kappa = 0.44 : \langle T \rangle = 23.3, \quad \langle U \rangle = 15.6, \quad \langle Y \rangle = 12.5 \text{ au.}$$

In the table below, we have summarized all the corrections and for comparison have also given the corresponding values obtained with a hydrogenic wave function.

	Hydrogenic wave function ($\kappa = 0$)	Modified hydrogenic wave functions	
		$\kappa = 0.40$	$\kappa = 0.44$
Landé value	1.14286	1.14286	1.14286
Schwinger correction	+0.00033	+0.00033	+0.00033
Breit-Margenau correction	-0.00166	-0.00134	-0.00126
Diamagnetic correction	-0.00084	-0.00070	-0.00066
Theoretical value	1.14069	1.14115	1.14127
Experimental value		1.14122 ± 0.00015	

It is seen that the agreement between the experimental and calculated g values is extremely good with κ around 0.4, the value obtained by comparison with SCF wave functions (see Appendix).

Since all wave functions used here are fitted to the experimental spin-orbit coupling constant with the same potential, the difference in result is entirely due to the difference in shape. The experimental deviation from the Landé value together with the spin-orbit coupling therefore constitutes a measure of the shape of the wave function. Although the accuracy here is not very high, it definitely shows that the hydrogenic wave function is too sharp. The hydrogenic wave function used above has been fitted to the experimental spin-orbit coupling constant by means of the Thomas-Fermi potential. If Z_{eff} is instead determined from Eq. (3) the agreement becomes even much poorer.

ACKNOWLEDGMENTS

We want to express our sincere thanks to Professor William A. Nierenberg for his inspiring guidance and interest in this work and particularly for the use of the computer program. The help of the reactor group at the Lawrence Radiation Laboratory, Livermore, and of the Health Chemistry division at this Laboratory is also acknowledged.

APPENDIX

Analytic Radial Wave Functions

For numerical calculations it is very convenient to have an approximate analytic expression for the wave functions obtained by the SCF method. This also makes it possible to interpolate between such functions. A suitable form is the Slater-Löwdin approximation,[15] which for functions of the 4f type (single maximum) is

$$R(r) = r^n(c_1 e^{-a_1 r} + c_2 e^{-a_2 r} + c_3 e^{-a_3 r} + \cdots).$$

With three terms in this expansion the agreement with the original wave function is extremely good. For our purpose, however, we prefer to use a two-parameter function, and choose the symmetric form

$$R(r) = N r^n e^{-ar} \cosh \kappa(ar-n) = \frac{1}{2} Nr^n(e^{-\kappa n} e^{-a(1-\kappa)r} + e^{\kappa n} e^{-a(1+\kappa)r}).$$

$$(A-1)$$

For this function the position of the maximum depends only on a, and the other parameter, κ, determines essentially the shape. A function of this type fitted to the SCF wave function for Tm^{3+} is shown in Fig. 6. One could easily determine both parameters in Eq. (A-1) by interpolation or extrapolation from existing SCF calculations, but we believe that more reliable wave functions are obtained if one of the parameters is determined from the experimental spin-orbit coupling constant. Since the shape of the wave function changes very little from element to element, we have determined κ by comparison with SCF wave functions and a from the spin-orbit coupling constant. In the latter case we have used the Thomas-Fermi potential, which is accurate enough for this purpose. This potential is particularly close to SCF potentials near the nucleus, where the main contribution to the spin-orbit coupling originates (see Fig. 7).

No SCF calculations are available for any rare earth atoms but some have recently been carried out for the Pr^{3+} and Tm^{3+} ions. [9] The difference in shape between the 4f wave functions for these ions is very small, and both correspond to a κ value slightly greater than 0.4. Since one would not expect the shape to differ much between the ions and the atoms, this should be a reasonable value also for the atoms. This is in agreement with the value obtained by extrapolation from heavier atoms like W and Hg.

For the wave function (A-1) the following formulas are easily verified (subscript hy indicates hydrogenic value).

$$N^2 = \frac{(2a)^{2n+1}}{(2n)!} \frac{1}{C_{2n+1}} = \frac{N_{hy}^2}{C_{2n+1}} \, ,$$

$$\left\langle r^{-m} \right\rangle = \frac{(2a)^m (2n-m)!}{(2n)!} \frac{C_{2n+1-m}}{C_{2n+1}} = \left\langle r^{-m} \right\rangle_{hy} \frac{C_{2n+1-m}}{C_{2n+1}} \, ,$$

$$\left\langle T \right\rangle = \frac{1}{2}\left[n(n-1)\left\langle r^{-2}\right\rangle - \left\langle \frac{1}{R}\frac{d^2 R}{dr^2}\right\rangle\right] = \frac{1}{2} a^2 \left[1 - \kappa^2 - 2\kappa \frac{D_{2n}}{C_{2n+1}}\right] \, ,$$

where

$$C_s = \frac{1}{4}\left[e^{-2n\kappa}(1-\kappa)^{-s} + 2 + e^{2n\kappa}(1+\kappa)^{-s}\right]$$

and

$$D_s = \frac{1}{4}\left[e^{-2n\kappa}(1-\kappa)^{-s} - e^{2n\kappa}(1+\kappa)^{-s}\right] \, .$$

REFERENCES

1. I. Lindgren, A. Cabezas, and W. A. Nierenberg, Bull. Am. Phys. Soc. II, 5, 273 (1960).

2. R. L. Graham, J. L. Wolfson, and R. E. Bell, Can. J. Phys. 30, 459 (1952).

3. W. F. Meggers, Revs. Modern Phys. 14, 96 (1942).

4. J. R. Zacharias, Phys. Rev. 61, 270 (1942);

   L. Davis, D. E. Nagle, and J. R. Zacharias, Phys. Rev. 76, 1068 (1949).

5. G. O. Brink, J. C. Hubbs, W. A. Nierenberg, and J. L. Worcester, Phys. Rev. 107, 189 (1957).

6. N. F. Ramsey, Molecular Beams (Oxford University Press, London, 1956).

7. R. Marrus, W. A. Nierenberg, and J. Winocur, Hyperfine Structure of Americium-241, UCRL-9207 (to be published).

8. L. Davis, B. T. Feld, C. W. Zabel, and J. R. Zacharias, Phys. Rev. 76, 1076 (1949).

9. E. C. Ridley, Proc. Cambridge Phil. Soc. 56, 41 (1960).

10. R. Sternheimer, Phys. Rev. 86, 316 (1952); Phys. Rev. 95, 736 (1954).

11. K. H. Lindenberger, Z. Physik 141, 476 (1955).

12. G. Breit, Nature 122, 649 (1928).

13. H. Margenau, Phys. Rev. 57, 383 (1940).

14. A. Abragam and J. H. Van Vleck, Phys. Rev. 92, 1448 (1953). More general treatments are given by K. Kembe and J. H. Van Vleck, Phys. Rev. 96, 66 (1954) and F. R. Innes and C. W. Ufford, Phys. Rev. 111, 194 (1958).

15. J. C. Slater, Phys. Rev. 42, 33 (1932); P. O. Löwdin, Phys. Rev. 90, 120 (1953).

FIGURE LEGENDS

Fig. 1. Schematic hfs energy-level diagram for Tm^{170}.

Fig. 2. Relative positions of the energy levels at zero field <u>versus</u> the

B/A ratio.

Fig. 3. Resonance frequencies divided by $\mu_0 H/h$ for the $\Delta F = 0$

transitions <u>versus</u> the magnetic field.

Fig. 4. Resonance curves for the $\Delta F = 0$ transitions and one $\Delta F = 1$

transition.

Fig. 5. Input and output data from the IBM 704 computer. The two

output sheets are obtained with opposite signs assumed for the

nuclear moment.

Fig. 6. Radial wave functions for Tm^{3+}.

Fig. 7. $r^2 \frac{dV}{dr}$ from the Thomas-Fermi potential and from SCF
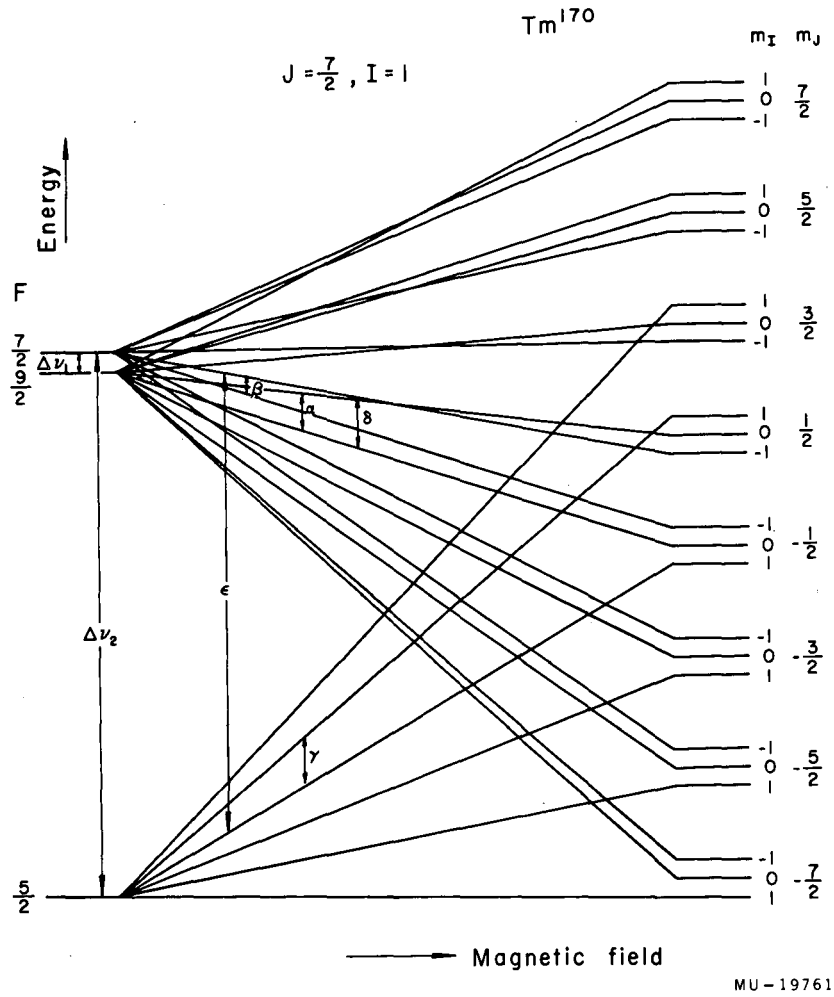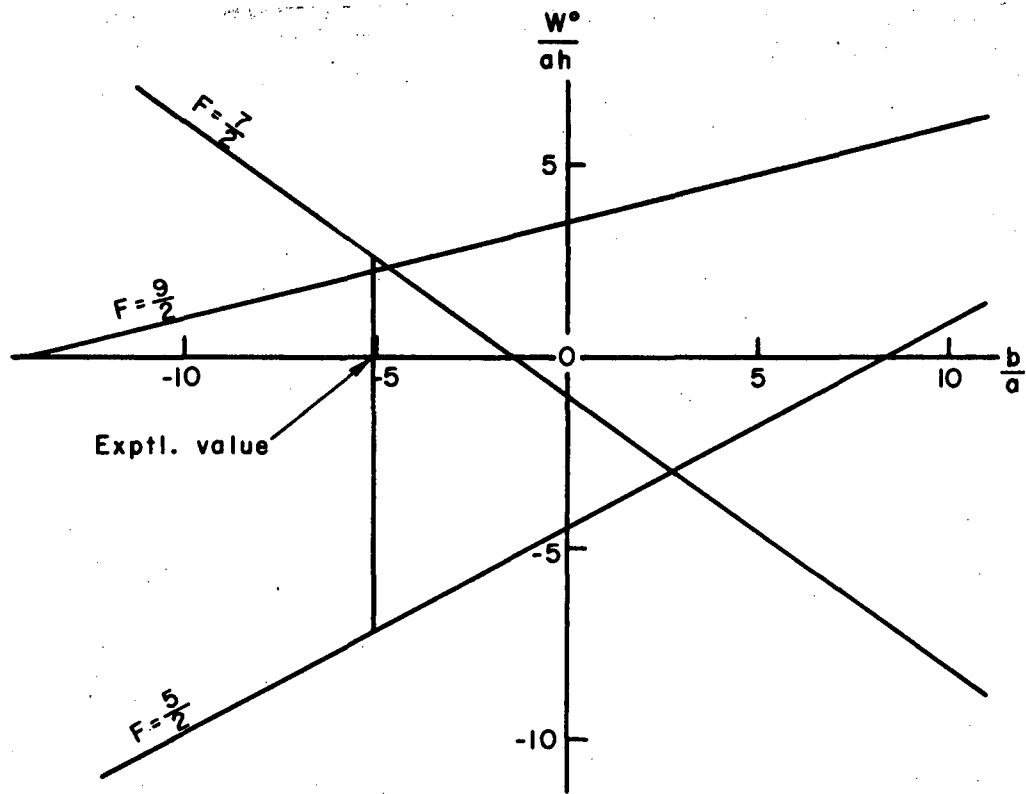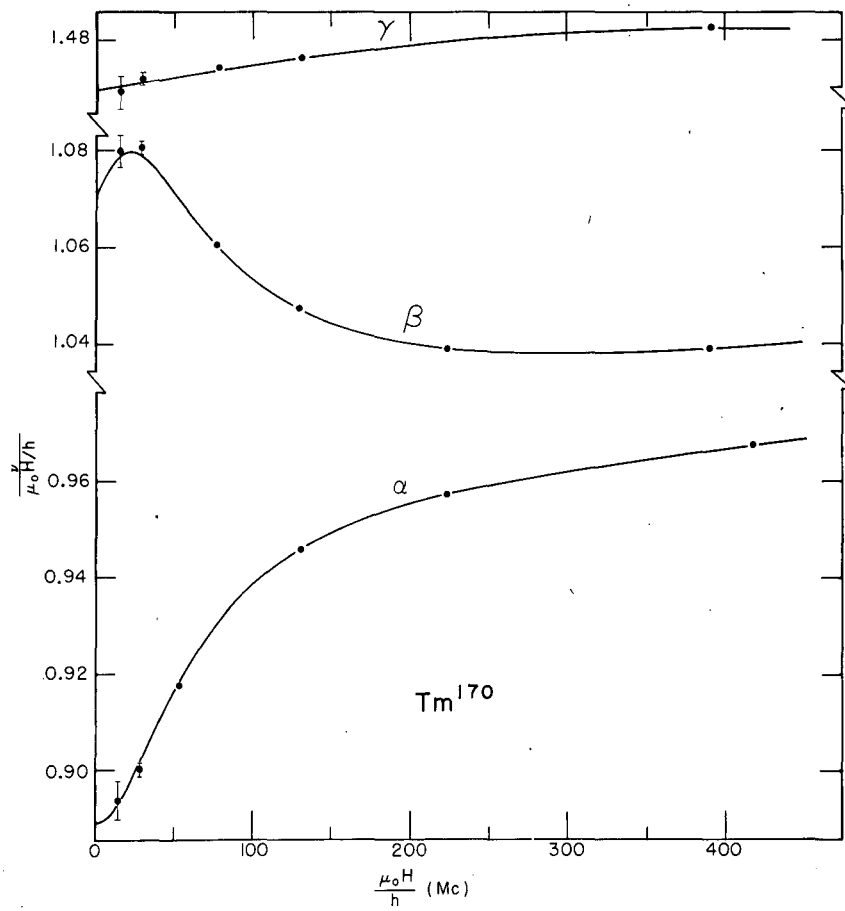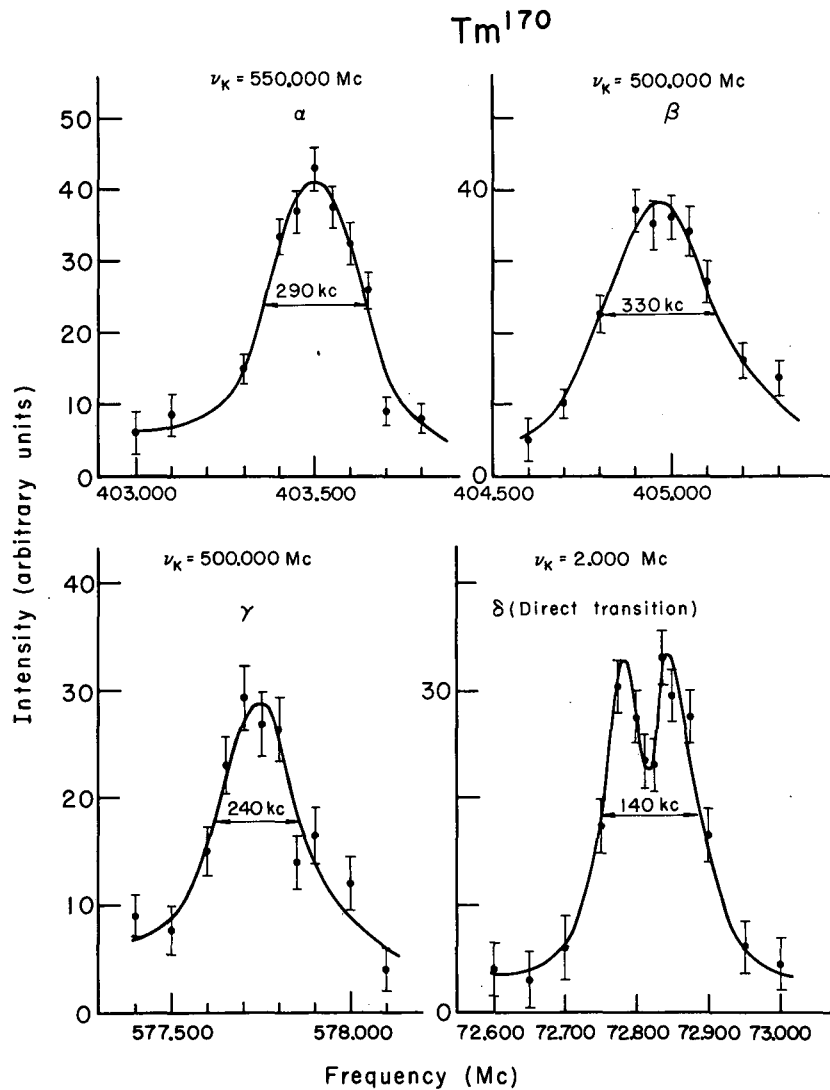
calculations in tungsten and mercury.

Fig. 1.

Fig. 2.

Fig. 3.

-22-

Fig. 4.

MAY. 7,1960

ISOTOPE TM170

I= 2/2 , J= 7/2

CABEZAS AND LINDGREN

COMPARING ISOTOPE 4

NAME	G	G X 10	A
	J	I	
TM169	-1.141200	+2.600000	-390.00000

CALIBRATING ISOTOPES 4

NAME	I	G	G X 10	DELTA
		J	I	NU
K39	+1.5	-2.002280	+1.419450	+461.71970

INPUT DATA

| | CALIBRATING ISOTOPE | | | | UNKNOWN ISOTOPE | | | | | | |

DATA NO.	NAME	FREQ. (MC/SEC)	FREQ. ERROR	FREQ. (MC/SEC)	FREQ. ERROR	F 1	M 1	F 2	M 2	H (GAUSS)	DELTA H (GAUSS)
1	K39	+.500	+.050	+.950	+.050	9/2	1/2	9/2	-1/2	+.711	+.071
2	K39	+1.000	+.050	+1.760	+.050	9/2	1/2	9/2	-1/2	+1.418	+.070
3	K39	+8.000	+.030	+13.600	+.070	9/2	1/2	9/2	-1/2	+10.865	+.039
4	K39	+16.000	+.050	+26.100	+.040	9/2	1/2	9/2	-1/2	+20.754	+.059
5	K39	+32.000	+.050	+49.070	+.030	9/2	1/2	9/2	-1/2	+38.243	+.050
6	K39	+100.000	+.050	+123.000	+.050	9/2	1/2	9/2	-1/2	+93.043	+.033
7	K39	+.500	+.050	+1.100	+.050	7/2	-1/2	7/2	-3/2	+.711	+.071
8	K39	+1.000	+.050	+2.125	+.050	7/2	-1/2	7/2	-3/2	+1.418	+.070
9	K39	+8.000	+.030	+16.400	+.050	7/2	-1/2	7/2	-3/2	+10.865	+.039
10	K39	+16.000	+.050	+31.350	+.050	7/2	-1/2	7/2	-3/2	+20.754	+.059
11	K39	+50.000	+.050	+81.830	+.040	7/2	-1/2	7/2	-3/2	+55.192	+.043
12	K39	+100.000	+.050	+136.150	+.060	7/2	-1/2	7/2	-3/2	+93.043	+.033
13	K39	+.500	+.050	+1.470	+.050	5/2	3/2	5/2	1/2	+.711	+.071
14	K39	+8.000	+.030	+22.310	+.050	5/2	3/2	5/2	1/2	+10.865	+.039
15	K39	+16.000	+.050	+42.700	+.030	5/2	3/2	5/2	1/2	+20.754	+.059
16	K39	+50.000	+.050	+113.745	+.040	5/2	3/2	5/2	1/2	+55.192	+.043
17	K39	+220.000	+.050	+213.460	+.060	9/2	1/2	9/2	-1/2	+159.545	+.024
18	K39	+220.000	+.050	+231.715	+.075	7/2	-1/2	7/2	-3/2	+159.545	+.024
19	K39	+500.000	+.050	+577.740	+.075	5/2	3/2	5/2	1/2	+278.798	+.020
20	K39	+500.000	+.050	+404.970	+.100	7/2	-1/2	7/2	-3/2	+278.798	+.020
21	K39	+550.000	+.050	+403.505	+.080	9/2	1/2	9/2	-1/2	+298.380	+.019
22	K39	+.520	+.030	+72.855	+.025	7/2	-1/2	9/2	-1/2	+.740	+.042
23	K39	+2.000	+.030	+72.815	+.025	7/2	-1/2	9/2	-1/2	+2.818	+.042
24	K39	+100.000	+.050	+192.010	+.060	5/2	3/2	5/2	1/2	+93.043	+.033

Fig. 5

MAGNETIC DIPOLE,ELECTRIC QUADRUPOLE AND G CONSTANTS

TM170

ITERATION NO.	MAGNETIC DIPOLE	ELECTRIC QUADRUPOLE	G J	ERROR IN A	ERROR IN B	ERROR IN G	CHI SQUARE
1	+200.300	-1011.200	-1.141199	+.0000	+.0000	+.0000	+4 +.20553567
2	+200.448	-1011.057	-1.141248	+1.9917	+9.2948	+.0001	+1 +.41455212
3	+200.447	-1011.051	-1.141249	+1.9964	+9.3167	+.0001	+1 +.41435036
4	+200.447	-1011.053	-1.141249	+2.0017	+9.3415	+.0001	+1 +.41438045

ENERGY LEVELS AND RESIDUALS

TM170

G = -.000134   U/H = +1.399677
I

DATA NO.	FREQ. (MC/SEC)	ENERGY LEVEL 1	ENERGY LEVEL 2	RESIDUALS	F 1	M 1	F 2	M 2	H (GAUSS)	DELTA H (GAUSS)	WEIGHT FACTOR
1	+.950	+449.238	+448.354	+.066	9/2	1/2	9/2	-1/2	+.711	+.071	+97.5
2	+1.760	+449.654	+447.892	-.002	9/2	1/2	9/2	-1/2	+1.418	+.070	+98.4
3	+13.600	+453.843	+440.281	+.038	9/2	1/2	9/2	-1/2	+10.865	+.039	+137.3
4	+26.100	+455.885	+429.728	-.057	9/2	1/2	9/2	-1/2	+20.754	+.059	+135.1
5	+49.070	+455.719	+406.638	-.011	9/2	1/2	9/2	-1/2	+38.243	+.050	+184.3
6	+123.000	+444.489	+321.458	-.030	9/2	1/2	9/2	-1/2	+93.043	+.033	+220.6
7	+1.100	+521.208	+520.144	+.035	7/2	-1/2	7/2	-3/2	+.711	+.071	+72.6
8	+2.125	+520.704	+518.579	-.000	7/2	-1/2	7/2	-3/2	+1.418	+.070	+73.2
9	+16.400	+515.462	+499.082	+.020	7/2	-1/2	7/2	-3/2	+10.865	+.039	+168.3
10	+31.350	+512.698	+481.409	+.060	7/2	-1/2	7/2	-3/2	+20.754	+.059	+96.6
11	+81.830	+515.745	+433.960	+.045	7/2	-1/2	7/2	-3/2	+55.192	+.043	+178.1
12	+136.150	+527.789	+391.623	-.016	7/2	-1/2	7/2	-3/2	+93.043	+.033	+170.4
13	+1.470	-1441.458	-1442.920	+.008	5/2	3/2	5/2	1/2	+.711	+.071	+42.2
14	+22.310	-1410.250	-1432.578	-.018	5/2	3/2	5/2	1/2	+10.865	+.039	+112.8
15	+42.700	-1379.972	-1422.647	+.025	5/2	3/2	5/2	1/2	+20.754	+.059	+63.7
16	+113.745	-1275.484	-1389.170	+.058	5/2	3/2	5/2	1/2	+55.192	+.043	+101.8
17	+213.460	+428.013	+214.493	-.059	9/2	1/2	9/2	-1/2	+159.545	+.024	+213.4
18	+231.715	+555.362	+323.612	-.036	7/2	-1/2	7/2	-3/2	+159.545	+.024	+146.2
19	+577.740	-637.221	-1214.913	+.048	5/2	3/2	5/2	1/2	+278.798	+.020	+137.1
20	+404.970	+613.438	+208.493	+.024	7/2	-1/2	7/2	-3/2	+278.798	+.020	+92.3
21	+403.505	+402.525	-1.005	-.026	9/2	1/2	9/2	-1/2	+298.380	+.019	+140.5
22	+72.855	+521.188	+448.335	+.002	7/2	-1/2	9/2	-1/2	+.740	+.042	+1570.3
23	+72.815	+519.750	+446.932	-.003	7/2	-1/2	9/2	-1/2	+2.818	+.042	+1589.6
24	+192.010	-1162.392	-1354.378	+.024	5/2	3/2	5/2	1/2	+93.043	+.033	+120.0

Fig. 5 continued

MAGNETIC DIPOLE,ELECTRIC QUADRUPOLE AND G CONSTANTS

TM170

ITERATION NO.	MAGNETIC DIPOLE	ELECTRIC QUADRUPOLE	G J	ERROR IN A	ERROR IN B	ERROR IN G	CHI SQUARE
1	+200.300	-1011.200	-1.141199	+.0000	+.0000	+.0000	+4 +.20548280
2	+199.750	-1007.800	-1.141222	+2.0131	+9.3949	+.0001	+1 +.33591194
3	+199.764	-1007.861	-1.141223	+1.9800	+9.2405	+.0001	+1 +.33312231
4	+199.764	-1007.861	-1.141223	+1.9904	+9.2886	+.0001	+1 +.33317843

ENERGY LEVELS AND RESIDUALS
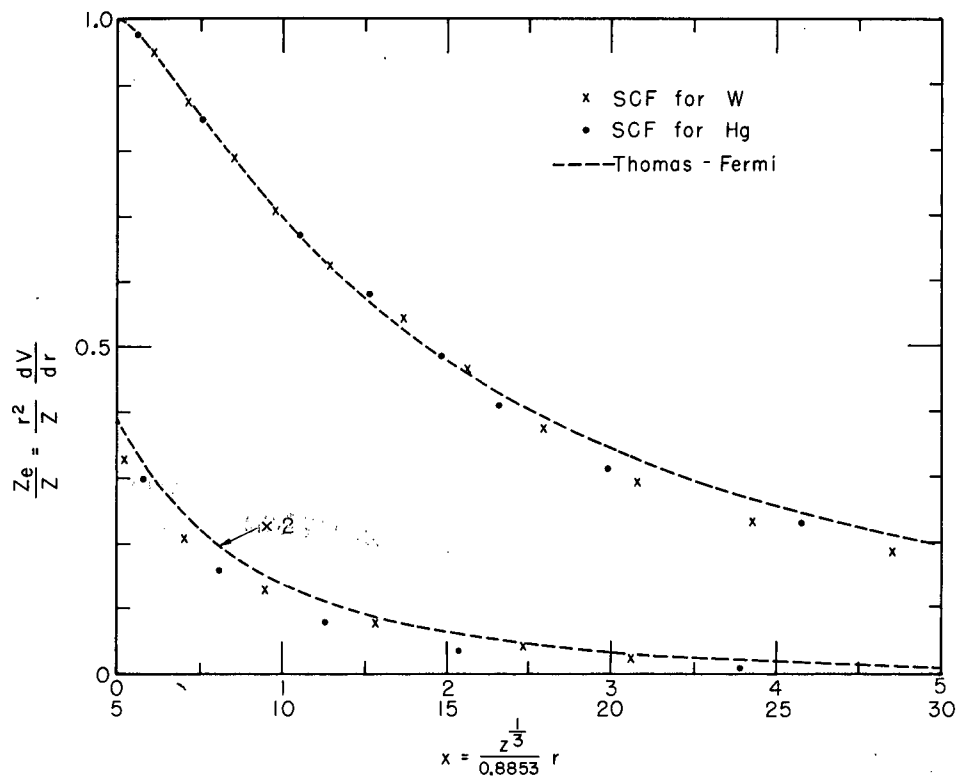
TM170

G = +.000133   U/H = +1.399677
I

DATA NO.	FREQ. (MC/SEC)	ENERGY LEVEL 1	ENERGY LEVEL 2	RESIDUALS	F 1	M 1	F 2	M 2	H (GAUSS)	DELTA H (GAUSS)	WEIGHT FACTOR
1	+.950	+447.642	+446.758	+.066	9/2	1/2	9/2	-1/2	+.711	+.071	+97.4
2	+1.760	+448.059	+446.296	-.002	9/2	1/2	9/2	-1/2	+1.418	+.070	+98.4
3	+13.600	+452.246	+438.686	+.039	9/2	1/2	9/2	-1/2	+10.865	+.039	+137.3
4	+26.100	+454.286	+428.130	-.055	9/2	1/2	9/2	-1/2	+20.754	+.059	+135.0
5	+49.070	+454.116	+405.039	-.007	9/2	1/2	9/2	-1/2	+38.243	+.050	+184.2
6	+123.000	+442.877	+319.856	-.021	9/2	1/2	9/2	-1/2	+93.043	+.033	+220.5
7	+1.100	+519.613	+518.547	+.035	7/2	-1/2	7/2	-3/2	+.711	+.071	+72.5
8	+2.125	+519.108	+516.983	+.000	7/2	-1/2	7/2	-3/2	+1.418	+.070	+73.1
9	+16.400	+513.868	+497.488	+.020	7/2	-1/2	7/2	-3/2	+10.865	+.039	+168.2
10	+31.350	+511.106	+479.818	+.061	7/2	-1/2	7/2	-3/2	+20.754	+.059	+96.5
11	+81.830	+514.167	+432.385	+.048	7/2	-1/2	7/2	-3/2	+55.192	+.043	+178.1
12	+136.150	+526.229	+390.066	-.012	7/2	-1/2	7/2	-3/2	+93.043	+.033	+170.4
13	+1.470	-1436.671	-1438.132	+.008	5/2	3/2	5/2	1/2	+.711	+.071	+42.2
14	+22.310	-1405.461	-1427.790	-.019	5/2	3/2	5/2	1/2	+10.865	+.039	+112.8
15	+42.700	-1375.184	-1417.859	+.024	5/2	3/2	5/2	1/2	+20.754	+.059	+63.6
16	+113.745	-1270.698	-1384.389	+.054	5/2	3/2	5/2	1/2	+55.192	+.043	+101.8
17	+213.460	+426.406	+212.900	-.045	9/2	1/2	9/2	-1/2	+159.545	+.024	+213.4
18	+231.715	+553.841	+322.092	-.034	7/2	-1/2	7/2	-3/2	+159.545	+.024	+146.2
19	+577.740	-632.625	-1210.334	+.030	5/2	3/2	5/2	1/2	+278.798	+.020	+137.1
20	+404.970	+611.997	+207.043	+.017	7/2	-1/2	7/2	-3/2	+278.798	+.020	+92.3
21	+403.505	+400.983	-2.533	-.011	9/2	1/2	9/2	-1/2	+298.380	+.019	+140.5
22	+72.855	+519.592	+446.740	+.002	7/2	-1/2	9/2	-1/2	+.740	+.042	+1570.3
23	+72.815	+518.155	+445.336	-.003	7/2	-1/2	9/2	-1/2	+2.818	+.042	+1589.6
24	+192.010	-1157.616	-1349.611	+.016	5/2	3/2	5/2	1/2	+93.043	+.033	+120.0

Fig. 5 continued

Fig. 6.

MU-20199

Fig. 7.